Structure of the liquid-vapor interface of a dilute alloy of Pb in Ga

Bin Yang, Dongxu Li, Zhengqing Huang, and Stuart A. Rice
Department of Chemistry and The James Franck Institute, The University of Chicago, Chicago, Illinois 60637
(Received 7 March 2000; revised manuscript received 17 July 2000)

We report the results of x-ray reflectivity and grazing-incidence x-ray diffraction studies of the liquid-vapor interfaces of three dilute lead-in-gallium alloys (0.16, 0.047, and 0.025 wt %) over the temperature range 23–76 °C. These experiments determine, respectively, the density distributions along the normal to the interface and the in-plane pair correlation functions. In this temperature range, at each of the alloy concentrations, the excess Pb in the interface forms a complete monolayer that is the outermost stratum of the interface. When the temperature is below 58 °C that Pb monolayer is in a two-dimensional hexagonal crystalline state, evidence for which is the appearance of four sharp peaks in the grazing-incidence x-ray diffraction pattern. The structural parameters of the hexagonal crystalline state are $\mathbf{a}=0.342$ nm and $\mathbf{b}=0.592$ nm, with **a** and **b** the basis vectors of a degenerate two-dimensional body-centered orthorhombic lattice. At about 58 °C the Pb monolayer undergoes a transition to a state with less order, evidence for which is the appearance of broadened diffraction peaks; the locations of the broadened and sharp diffraction peaks are the same. The nearly discontinuous change in the range of positional order at the transition temperature, coupled with the lack of change of the positions of the diffraction peaks, suggest that this transition is first order with either very small or zero density change. Our data cannot determine if the disordered phase is liquid or hexatic. An analogy between the character of the observed transition and the first-order melting transition in a one-component two-dimensional classical plasma is suggested.

I. INTRODUCTION

The existence of a composition difference between the liquid-vapor interface and the bulk liquid phase of a binary mixture has been known since the work of Gibbs (see, e.g., Ref. 1). However, it is only in the last few years that information about the atomic structure of that interface has become available. The results of recent studies reveal that the structures of the liquid-vapor interfaces of ordinary binary liquid mixtures and of binary liquid metal alloys are different.[2–13] Theoretical studies of the liquid-vapor interface of an ordinary liquid mixture predict that at temperatures not far from the freezing point the density varies smoothly along the normal to the interface. It is found that the density falls monotonically from the value characteristic of the bulk liquid to that characteristic of the vapor over a distance of approximately two molecular diameters. Furthermore, the concentration of the species in excess in the interface is predicted to vary slowly across the interface. The corresponding theoretical predictions for the liquid-vapor interfaces of binary liquid metal alloys are, first, that the (longitudinal) distribution of density along the normal to the interface is stratified for several atomic diameters into the bulk liquid, and, second, that the species in excess in the interface forms a monolayer that is the outermost layer of that interface. Recent x-ray reflectivity (XR) and grazing-incidence x-ray diffraction (GIXD) studies of the liquid-vapor interfaces of several binary liquid metal alloys have confirmed these predictions.[14–28]

An understanding of the differences between the structures of the liquid-vapor interfaces of ordinary binary liquid mixtures and of binary liquid metal alloys follows from the observation that the liquid-vapor interface is a strongly inhomogeneous domain.[5,6] Moreover, the scale lengths that define the properties of that domain, namely, the interface width, the range of order perpendicular to its normal, the depth over which the excess concentration of the segregated component is distributed, and the range of the molecular interactions, are of comparable magnitudes. The differences between the structures of the liquid-vapor interfaces of ordinary binary liquid mixtures and binary liquid metal alloys are signatures of the responses of the systems to the density dependence of the interactions in the interface. Since the density dependence of a van der Waals type interaction is rather weak, to a very good approximation there is no change in the pair potential along the density gradient in the liquid-vapor interface of an ordinary liquid mixture. In contrast, for a binary liquid metal alloy, the electron density changes from the value characteristic of the bulk liquid to zero across the liquid-vapor interface and, over the same distance, the electrons undergo a transition from being delocalized (in the bulk liquid) to localized (in the vapor). Accordingly, the effective ion-ion interaction, which is strongly electron density dependent, changes considerably as the interface is traversed from the bulk liquid to the vapor. When the pseudopotential representation of the free-energy density of the liquid metal is used, it is the density variation of the so-called structure-independent energy that drives the stratification of the liquid-vapor interface.

As already noted, the segregation of, say, the solute in the liquid-vapor interface of a dilute binary liquid metal alloy usually results in the formation of a monolayer that is the outermost layer of that interface. The experimental evidence available to date, for dilute solutions of bismuth in gallium,[26,27] indium in gallium,[21] and tin in gallium,[28] indicates that the segregated layer has the structure of a quasi-two-dimensional liquid. The results of self-consistent quantum Monte Carlo simulations of the liquid-vapor interfaces of these alloys, and others, support this conclusion. Neither the experimental data nor the results of the simulations de-

fine the range of temperature in which the segregated monolayer remains a quasi-two-dimensional liquid.

It is not at all clear what one should expect for the structure of the segregated layer in the liquid-vapor interface of a binary alloy. In the systems studied to date, the three-dimensional crystalline forms of the species that form the monolayers melt at temperatures that are much higher than the temperatures at which the liquid binary alloys are studied. We suggest that it is not unreasonable to expect that at a suitable temperature the segregated layer will undergo a freezing transition to a quasi-two-dimensional ordered solid. Put another way, it may be possible to use the liquid-vapor interface of a suitably chosen alloy to study phase transitions in a quasi-two-dimensional system. Execution of such a study will depend on finding a system in which there is a fortuitous balance between the ion-ion interactions in the alloy and thermal excitations so that there is an accessible experimental window that can be used for observations.

In this paper we report the results of XR and GIXD studies of the liquid-vapor interfaces of three dilute alloys of Pb in Ga, over the temperature range 23–76 °C. As in the other dilute alloy systems studied, it is found that the excess Pb in the liquid-vapor interface forms a monolayer that is the outermost stratum of that interface. When the temperature is below 58 °C that Pb monolayer is in a two-dimensional hexagonal crystalline state, evidence for which is the appearance of four sharp peaks in the grazing-incidence x-ray diffraction pattern. The structural parameters of the hexagonal crystalline state are $\mathbf{a}=0.342$ nm and $\mathbf{b}=0.592$ nm, with **a** and **b** the basis vectors of a degenerate two-dimensional body-centered orthorhombic lattice. At about 58 °C the Pb monolayer undergoes a transition to a state with less order, evidence for which is the appearance of broadened diffraction peaks; the locations of the broadened and sharp diffraction peaks are the same. The nearly discontinuous change in the range of positional order at the transition temperature, coupled with the lack of change of the positions of the diffraction peaks, suggest that this transition is first order with either very small or zero density change. Our data cannot determine if the disordered phase is liquid or hexatic. We suggest an interpretation of our observations using an analogy between the character of the observed transition and the first-order melting transition in a one-component two-dimensional classical plasma.

II. EXPERIMENTAL DETAILS

The high-vacuum sample chamber used for our experiments has been described elsewhere,[25–28] as has the x-ray surface scattering spectrometer and the detection electronics used. We merely note that the sample chamber contains a residual gas analyzer to monitor the vacuum, an Auger spectrometer to monitor the liquid sample surface composition, and an ion gun and a sweep arm to clean the liquid sample surface.

Three samples of dilute Pb-in-Ga alloys were prepared as follows. In each case a weighed amount of Pb plate (1 mm thickness, 99.9995%, Alfa Chemicals) was added to 500 g of liquid Ga (99.999 99% Alfa Chemicals). The highest-concentration sample was made by adding 3.5 g of Pb to the Ga in a small vacuum chamber held at a pressure of

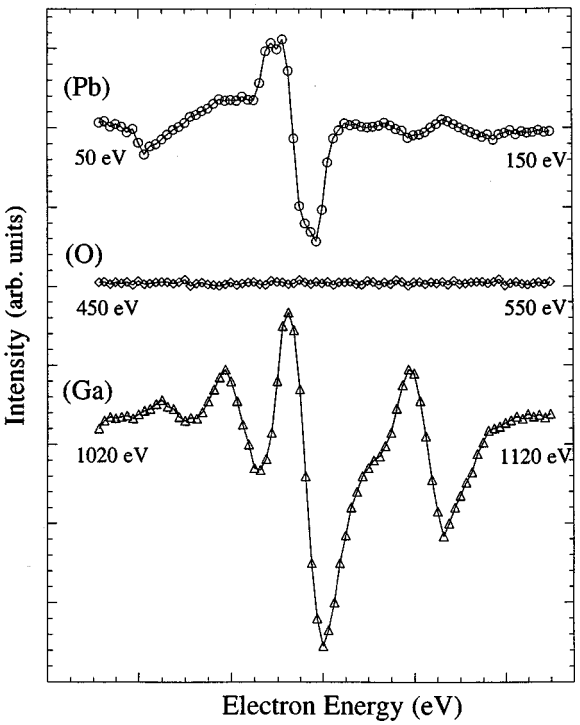

FIG. 1. Typical Auger spectra of the liquid-vapor interface of a PbGa alloy, with a primary beam energy of 3 keV. These data clearly show the presence of lead and gallium, and the absence of oxygen, in the liquid-vapor interface.

10^{-6} torr. The sample was maintained at 250 °C for about 12 h. After cooling to 60 °C, it was found that there was Pb at the bottom of the chamber, clearly indicating that the mixture was a saturated solution of Pb in Ga. Two lower-concentration samples, made by adding 0.35 and 0.20 g of Pb to 500 g of Ga, respectively, were prepared by stirring the mixture for 12 h at about 200 °C in a beaker filled with argon gas. In both instances the Pb dissolved completely in the Ga host liquid. The concentrations of Pb in the alloy samples (at room temperature) were determined, after completion of the experiments, by atomic absorption spectroscopy. The three samples studied had Pb concentrations of 0.16, 0.047, and 0.025 wt %,[29] respectively.

After preparation, a 300 g sample of the alloy was transferred, under an argon atmosphere at about 50 °C, to the reservoir attached to the ultrahigh-vacuum x-ray chamber. The alloy was fed into the sample cell in the x-ray chamber via a capillary attached to that reservoir while the background pressure in the chamber was maintained at 3×10^{-10} torr. The liquid surface was then sputtered (3 KV, 20 mA) for 24 h using an Ar ion gun, and examined by Auger spectroscopy. In addition to the signal from Ga, the Auger spectrum of the liquid alloy surface revealed the expected presence of excess Pb, and also clearly indicated the absence of any oxides (Fig. 1). Analysis of the composition of the residual gas over the sample showed that the partial pressure of oxygen was less than 10^{-12} torr. Both XR and GIXD measurements usually started about 24 h after the liquid sample was introduced into the chamber. All of our XR and GIXD experiments were carried out with a background pressure around 3×10^{-10} torr.

Our XR and GIXD measurements were carried out at

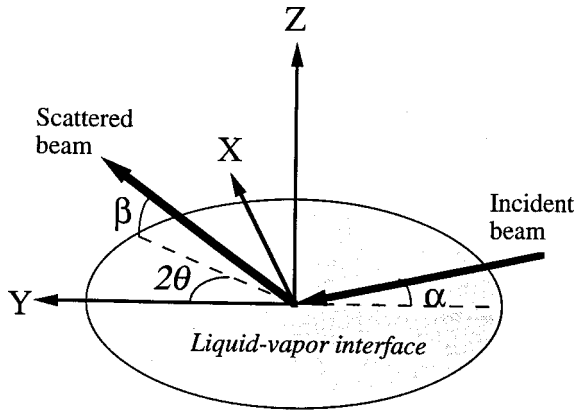

FIG. 2. Sketch of the incident and scattered x-ray paths in the experimental apparatus.

beamline X19C, at the National Synchrotron Light Source, Brookhaven National Laboratory. The x-ray wavelength used was 0.700 Å. The XR and GIXD measurements were carried out at many temperatures between 23 and 76 °C, with multiple cycling of the temperature up and down over this range.

Figure 2 shows a sketch of the x-ray paths in the experimental arrangement. Since the critical angle for total external reflection of the x rays by our samples is about 0.15°, the angle of incidence chosen for the GIXD measurements was $\alpha = 0.1°$; the pick-off angle of the detector was $\beta = 0.1°$. The GIXD measurements covered the angular range from $5° < 2\theta < 40°$. To measure the x-ray scattering from the bulk liquid alloy we used $\alpha = \beta = 0.25°$. At this angle of incidence the penetration depth[30] of the x rays is large enough (about 100 nm) that the intensity of the scattering from the liquid-vapor interface is negligible relative to the intensity of scattering from the bulk liquid. Since the alloys studied have very low Pb concentrations, we can attribute the bulk scattering to pure liquid Ga, and use those data for background subtraction.

It is necessary to comment briefly on the temperatures quoted in this paper. The temperature of the liquid alloy was controlled by circulating thermostated water through a coil that is in thermal contact with the sample cell through the chamber wall. The temperature of the sample cell is not identical with the temperature of the thermostated water. Our calibration of this temperature difference is only modestly accurate, so the temperatures quoted must be understood to be approximations to the true temperature. However, our calibrations do establish that the temperature of the sample cell monotonically tracks the temperature of the thermostated water, so that all of the temperature-dependent trends in the experimental data are valid. In particular, the existence of a phase transition in the segregated layer of Pb in the liquid-vapor interface of the PbGa alloy is established, albeit the temperature at which the transition occurs, which we cite as 58 °C, is uncertain by up to ten degrees Celsius.

III. EXPERIMENTAL RESULTS

A. X-ray reflectivity

Figure 3 displays the x-ray reflectivity as a function of q_z for the three alloys studied when the temperature is 28 °C

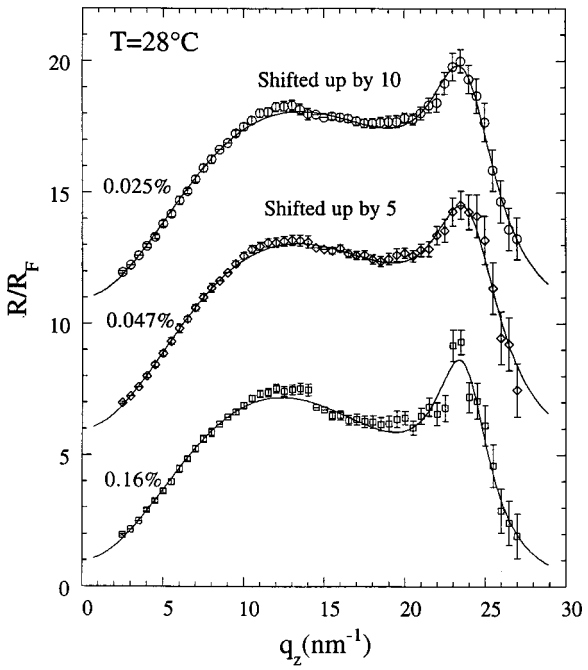

FIG. 3. X-ray reflectivity as a function of q_z for the three dilute PbGa alloys studied. The data have been normalized to the Fresnel reflectivity from the interface. The lines indicate the best fit of the reflectivity for the model longitudinal density profiles shown in Figs. 5 and 6 below.

(23 °C for the 0.047% alloy). Figure 4 displays the reflectivity as a function of q_z at three different temperatures for the alloy that contains 0.025 wt % Pb. These data show clearly that the reflectivity varies very little with alloy composition

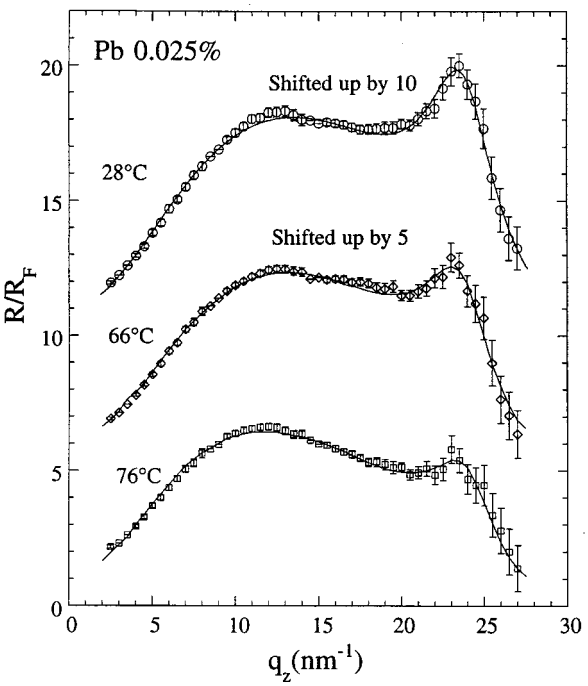

FIG. 4. X-ray reflectivity as a function of q_z and of temperature for the 0.025 wt % PbGa alloy. The data have been normalized to the Fresnel reflectivity from the interface. The lines indicate the best fit of the reflectivity for the model longitudinal density profiles shown in Figs. 5 and 6 below.

at a fixed temperature, and that it varies systematically with temperature at a fixed alloy composition. Our analysis of these data is described below.

The reflectivity of x rays incident on a sample of matter is sensitive to the electron density distribution perpendicular to the surface. Using the Born approximation, it can be shown that[31]

$$R(q_z)=R_F(q_z)\exp[-\sigma_{\rm cw}^2 q_z^2]|\Phi(q_z)|^2,$$

$$\Phi(q_z)=\frac{1}{\rho_{\rm el}(\infty)}\int_{-\infty}^{\infty}\frac{d\langle_{\rm el}(z)\rangle}{dz}e^{iq_z z}, \tag{3.1}$$

with $\rho_{\rm el}(\infty)$ the electron density of the bulk liquid, $R_F(q_z)$ the Fresnel reflectivity for that electron density, and the exponential damping term representing the influence of capillary waves with mean square amplitude

$$\sigma_{\rm cw}^2=\frac{k_B T}{2\pi\gamma}\ln\left(\frac{k_{\rm max}}{k_{\rm min}}\right). \tag{3.2}$$

In Eq. (3.2), γ is the surface tension, and $k_{\rm max}$ and $k_{\rm min}$ are the magnitudes of the maximum and minimum wave vectors associated with the spectrum of capillary waves. The value of $k_{\rm max}$ is approximately π/a, where a is the nearest-neighbor spacing of the atoms; the value of $k_{\rm min}$ is determined by the size of the sample or, more usually, by the instrumental resolution. The magnitude of the wave vector corresponding to the critical angle for total external reflection of x rays from pure liquid Ga has the value 0.481 $\rm nm^{-1}$.

Direct inversion of Eq. (3.1) to yield the longitudinal density profile is not possible because of the lack of phase information in the reflectivity data. We proceed, as we did in previous papers, and as have other investigators, to fit a plausible model to the longitudinal density profile. Specifically, we have analyzed our reflectivity data using two versions of the distorted crystal model introduced by Magnussen *et al.*[14,32] In the first version we assume that the excess Pb atoms segregated in the liquid-vapor interface of the alloy are only in the outermost stratum of that interface. The model is then defined by the liquid-vapor interface density distributions

$$\frac{\rho_{\rm Pb}(z)}{\rho_{\rm Ga}(\infty)}=\frac{\alpha d}{(2\pi)^{1/2}\sigma_0}\exp\left[-\frac{(z+d_1)^2}{2\sigma_0^2}\right],$$

$$\frac{\rho_{\rm Ga}(z)}{\rho_{\rm Ga}(\infty)}=\sum_{j=0}^{\infty}\frac{d}{(2\pi)^{1/2}\sigma_j}\exp\left[-\frac{(z-jd)^2}{2\sigma_j^2}\right], \tag{3.3}$$

$$\sigma_j^2=\sigma_0^2+(j+1)\sigma^2.$$

In Eqs. (3.3), $\rho_{\rm Ga}(\infty)$ is the atomic density of bulk liquid gallium, α is the ratio of the number density of the Pb layer to that of a Ga layer, d_1 is the separation of the Pb and Ga layers, and d is the distance between Ga layers. Note that the layers become increasingly roughened with increasing penetration into the liquid. The roughness of each layer is represented by the sum of an intrinsic component common to each layer, σ_0^2, and a component that increases as j increases, $(j+1)\sigma^2$. For the alloys we have studied, the concentration of Pb in the bulk liquid is so small that, to an excellent approximation, the bulk liquid can be considered to be pure Ga.

The longitudinal electron density in the liquid-vapor interface is obtained from the convolution of the longitudinal atomic density and the electronic density of each atom:[19]

$$\rho_{\rm el}(z)=\frac{\alpha d}{(2\pi)^{1/2}\sigma_0}\exp\left[-\frac{(z+d_1)^2}{2\sigma_0^2}\right]\otimes f_{\rm Pb}(z)$$
$$+\sum_{j=0}^{\infty}\frac{d}{(2\pi)^{1/2}\sigma_j}\exp\left[-\frac{(z-jd)^2}{2\sigma_j^2}\right]\otimes f_{\rm Ga}(z). \tag{3.4}$$

The predicted reflectivity, as a function of q_z, is

$$\frac{R(q_z)}{R_F(q_z)}=\frac{d^2}{f_{\rm Ga}^2(0)}q_z^2\exp[-\sigma_{\rm Pb}^2 q_z^2]\left|\alpha f_{\rm Pb}(q_z)\right.$$
$$\left.\times\exp[-iq_z d_1]+\frac{f_{\rm Ga}(q_z)}{\exp[\sigma^2 q_z^2/2]-\exp[iq_z d]}\right|^2. \tag{3.5}$$

In Eq. (3.5), $f_{\rm Ga}(q_z)$ and $f_{\rm Pb}(q_z)$ are the atomic scattering factors of Ga and Pb, and $\sigma_{\rm Pb}^2=\sigma_0^2+\sigma_{\rm cw}^2$.

The model just described assumes that the excess Pb that is in the liquid-vapor interface of a dilute Pb-in-Ga alloy is present in only the outermost stratum of that interface. To test that assumption, we have considered another distorted crystal model, in which the excess Pb atoms are allowed to be present also in the other layers of the stratified liquid-vapor interface of the alloy. We have examined two model distributions of the excess Pb atoms across the layers in the liquid-vapor interface. In one the concentration of Pb in each layer of the liquid-vapor interface is an independent variable;[28] in the other the concentration of Pb decreases exponentially as the distance into the bulk liquid increases. The fit of the experimental data to the latter model was found to be much more stable than the fit to the former model, so only the latter is discussed in this paper. It is defined by the longitudinal density distributions

$$\frac{\rho_{\rm Pb}(z)}{\rho_{\rm Ga}(\infty)}=\frac{\alpha d}{(2\pi)^{1/2}\sigma_0}\exp\left[-\frac{(z+d_1)^2}{2\sigma_0^2}\right]$$
$$+\sum_{j=0}^{\infty}\frac{x_{{\rm Pb},j}d}{(2\pi)^{1/2}\sigma_j}\exp\left[-\frac{(z-jd)^2}{2\sigma_j^2}\right],$$

$$\frac{\rho_{\rm Ga}(z)}{\rho_{\rm Ga}(\infty)}=\sum_{j=0}^{\infty}\frac{x_{{\rm Ga},j}d}{(2\pi)^{1/2}\sigma_j}\exp\left[-\frac{(z-jd)^2}{2\sigma_j^2}\right], \tag{3.6}$$

$$\sigma_j^2=\sigma_0^2+(j+1)\sigma^2.$$

By construction, the mole fraction of Pb decays exponentially as j increases. Then

$$x_{{\rm Pb},j}=c+(1-c)\exp[-(j+1)d/\xi_1],$$

$$x_{{\rm Ga},j}=(1-c)\{1-\exp[-(j+1)d/\xi_1]\}, \tag{3.7}$$

TABLE I. Best-fit parameters for model 1.

	Temperature range	
	23–56 °C	66–76 °C
α	0.725±0.001	0.721±0.003
σ (Å)	0.46±0.01	0.45±0.02
d_1 (Å)	2.59±0.02	2.62±0.05
d (Å)	2.583±0.005	2.60±0.01
ξ (Å)	4.4±0.2	4.6±0.5

TABLE II. Best-fit parameters for model 2.

	Temperature range	
	23–56 °C	66–76 °C
α	0.719±0.001	0.724±0.003
ξ_1 (Å)	0.71±0.01	0.81±0.02
σ (Å)	0.466±0.005	0.47±0.01
d_1 (Å)	2.55±0.01	2.51±0.02
d (Å)	2.552±0.003	2.53±0.01
ξ (Å)	4.1±0.1	3.9±0.2

where c is the mole fraction of Pb in the bulk liquid alloy, and ξ_1 is the concentration decay length. The predicted x-ray reflectivity as a function of q_z is now

$$\frac{R(q_z)}{R_F(q_z)}=\frac{d^2q_z^2\exp[-\sigma_{\mathrm{Pb}}^2q_z^2]}{[(1-c)f_{\mathrm{Ga}}(0)+cf_{\mathrm{Pb}}(0)]^2}\left|\alpha f_{\mathrm{Pb}}(q_z)\times\exp[-iq_zd_1]+\frac{(1-c)f_{\mathrm{Ga}}(q_z)+cf_{\mathrm{Pb}}(q_z)}{\exp[\sigma^2q_z^2/2]-\exp[iq_zd]}+\frac{(1-c)[f_{\mathrm{Pb}}(q_z)-f_{\mathrm{Ga}}(q_z)]}{\exp[(\sigma^2q_z^2/2)+(d/\xi_1)]-\exp[iq_zd]}\right|^2. \tag{3.8}$$

If the outermost stratum of the liquid-vapor interface is a two-dimensional ordered solid (see Sec. III), its atomic density can be determined from GIXD measurements. Then, with the density of this layer known, the density of the bulk liquid can be related to the parameters α and d. We have calculated the density of the bulk liquid alloy using the parameters obtained from the unconstrained fits of Eq. (3.8) to the x-ray reflectivity measurements. It is found that the simple distorted crystal model[26] implies that the bulk liquid density is about 7.0×10^3 kg/m^3, which is 15% higher than the known density of pure liquid gallium, namely, 6.095×10^3 kg/m^3. We consider this difference to be too large to be ignored. Accordingly, we have used the known value of the bulk liquid density as a constraint in the fit of Eq. (3.5) to the experimental data. This constraint was applied via the requirement that $\alpha d=\rho_{\mathrm{Pb,2D}}/\rho_{\mathrm{Ga,3D}}$, where $\rho_{\mathrm{Pb,2D}}$ is the two-dimensional (2D) number density of the Pb monolayer, and $\rho_{\mathrm{Ga,3D}}$ is the 3D number density of liquid Ga. $\rho_{\mathrm{Pb,2D}}$ is taken to be $\sqrt{3}q_{11}^2/(8\pi^2)$, where q_{11} is the wave vector of the (11) GIXD diffraction peak. We note that, for the very dilute alloys we have studied, the bulk liquid density is negligibly different from the density of pure liquid Ga.

The best-fit values of the parameters in Eq. (3.5) are displayed for both models in Tables I and II. Except for σ_{Pb}, the square of which increases linearly with increasing temperature,[31] none of the parameters in Eq. (3.5) are temperature dependent, hence only the average values in the low- and high-temperature phases (see below) are tabulated. Samples of the fits of the calculated reflectivity to the experimental data for the three alloys studied are shown in Figs. 3 and 4. The corresponding density profiles are shown in Figs. 5 and 6. The inferred temperature dependence of σ_{Pb}^2 is consistent with the predictions of capillary wave theory (see Fig. 7). The fact that the other parameters of the fitted profiles are sensibly temperature independent suggests that the surface layering does not change in the temperature range studied.

We note that the value of d inferred from our data is slightly larger than that inferred by Regan *et al.*[16] for pure gallium (2.552±0.003 versus 2.504±0.006 Å). There are several possible sources for this difference. At one extreme, it may signal the existence of a very small change in the lamellar structure of the Ga adjacent to the Pb monolayer in the alloy liquid-vapor interface relative to that in the pure Ga liquid-vapor interface. At a different extreme, it may signal the existence of a small systematic difference between the data sets coupled with the influence of experimental uncertainties on the parameters of the fit. The real origin of the difference, which is unknown to us, likely is some combination of the above.

Since the effective diameter of a Pb atom in pure lead is larger than that of a Ga atom in pure gallium, it is reasonable to expect that d_1 will be larger than d. However, in the liquid-vapor interface of the alloy the electron density is not the same as in either pure lead or gallium, and the effective atomic diameters will be sensitive to the local electron density. In fact, our fits to the experimental data yield the result

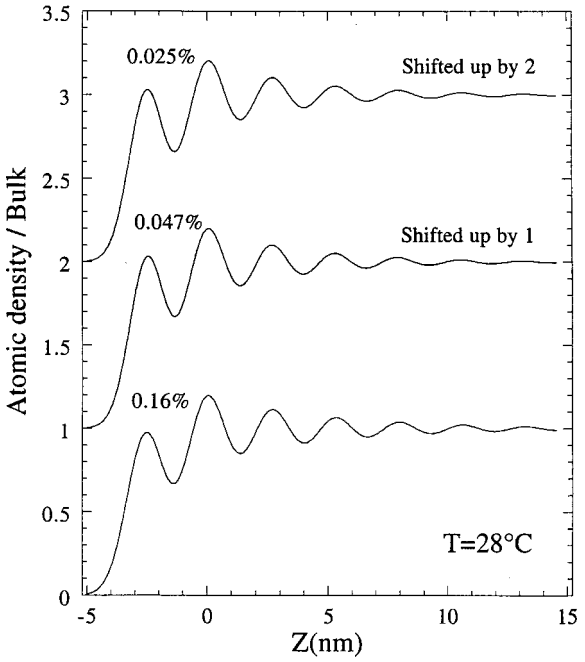

FIG. 5. The model longitudinal density profiles that fit the x-ray reflectivity data for the three alloys at 28 °C (23 °C for the 0.047% alloy).

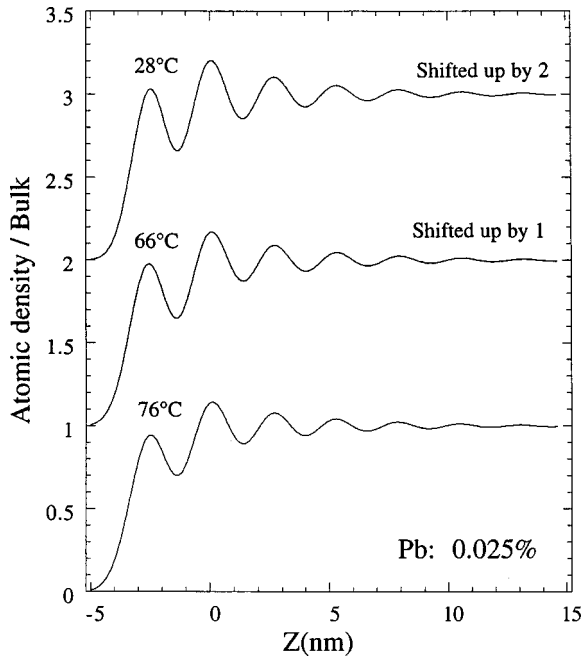

FIG. 6. The model longitudinal density profiles that fit the x-ray reflectivity data for the 0.025 wt % PbGa alloy at several temperatures.

that $d_1 = d$ to within the precision of the data.

The concentration decay length ξ_1 is found to be much smaller than the layer spacing, so that the concentration of Pb in the second layer of the interface is very small, only a few percent, and it is completely negligible in the deeper layers of the interface. We conclude that the representation of the liquid-vapor interface of the alloy as a stratified medium with the outer layer pure Pb and no Pb in the deeper layers is valid. We note that the value of ξ_1 found in our studies is similar to that found by Regan *et al.*[19] for the liquid-vapor interface of a Ga-In alloy.

The decay length for the density oscillations in the liquid-vapor interface, obtained using the known bulk density as a constraint on the fit, is found to be $\xi = 4.1 \pm 0.1$ Å. For the liquid-vapor interface of pure Ga, Regan *et al.* report the value $\xi = 5.3 \pm 0.1$ Å.[16]

When the fit of the density profile to the reflectivity data was not constrained to yield the known bulk density, we found that the fractional surface coverage by the excess Pb in the liquid-vapor interface decreased slightly as the temperature increased. This behavior is similar to that reported by Lei, Huang, and Rice[26] for the outermost layer of the liquid-vapor interface of a dilute Bi-in-Ga alloy, also obtained from a fit of the density profile that is not constrained to yield the correct bulk liquid Ga density. On the other hand, when the fit of the density profile to the reflectivity data is constrained to yield the known bulk density we find that the coverage keeps nearly the same value throughout our temperature range. This result is consistent with the fact (see below) that there is no detectable change in the positions of the peaks in the grazing-incidence diffraction pattern for the temperature range covered. Using the method suggested by Lei, Huang, and Rice,[26,28] the effective diameter of a Ga atom is calculated to be 2.87 Å, which is slightly larger than the value they obtained (2.78 Å).

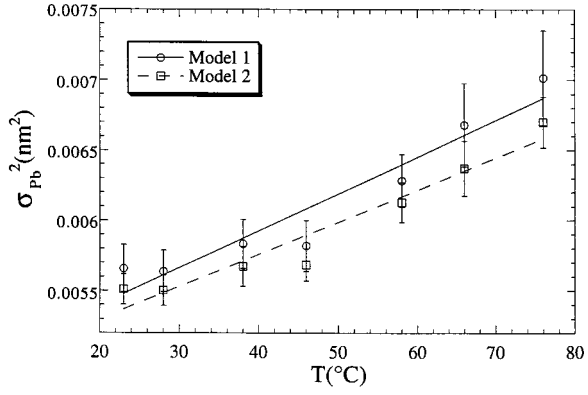

FIG. 7. The temperature dependence of σ_{Pb}^2 for the 0.025 wt % PbGa alloy. Results for the two model analyses of the reflectivity are shown.

B. Grazing-incidence x-ray diffraction

The geometric arrangement of the x-ray spectrometer is different for reflectivity and grazing-incidence diffraction measurements. Consequently, the XR and GIXD measurements were carried out separately on the same sample, over the same temperature range, but not at precisely the same temperatures. Examples of the GIXD intensity distribution from the liquid-vapor interface of Pb-in-Ga alloys, collected at temperatures 28, 66, and 76 °C, and without correction for the polarization of the incident x rays, are shown in Figs. 8(a)–8(c). At all of the temperatures in this range the diffraction patterns have a broad peak (centered at 25.3 nm^{-1}) arising from scattering by liquid Ga. Subtraction of the Ga scattering and the diffuse background scattering arising from the chamber[27] from the total GIXD scattering yields the results shown in Figs. 8(a)–8(c). These diffraction patterns are reproducible under cycling of the temperature of the sample and from sample to sample.

When the temperature is below 56 °C [see Fig. 8(a)], the GIXD pattern has four sharp peaks within the measured q_{xy} range, corresponding to d spacings of 0.296, 0.171, 0.148, and 0.112 nm. We attribute these diffraction peaks to scattering by an ordered array of Pb atoms. The character of the diffraction pattern indicates that the Pb atoms in the liquid-vapor interface form a two-dimensional hexagonal lattice. For convenience we choose to index the peaks observed in the basis of a degenerate two-dimensional body-centered orthorhombic lattice with $\mathbf{a} = 0.342$ nm and $\mathbf{b} = 0.592$ nm. In this basis the peaks are indexed as the (11), (20), (22), and (31) reflections, respectively. In this two-dimensional crystalline monolayer the nearest-neighbor separation is 0.342 nm, which is about 2% smaller than the nearest-neighbor separation in bulk crystalline Pb (0.350 nm). Our measurements also show that the intensities of the (11) and (20) diffraction peaks can be very much larger in magnitude (as much as 100-fold) than the maximum intensity of the broad peak in the diffraction pattern of liquid Ga.

The full width at half maximum (FWHM) of the (11) reflection is approximately equal to the angular resolution of the spectrometer as we used it. This observation implies that the correlation length for translational order in the two-dimensional hexagonal lattice, which is likely determined by

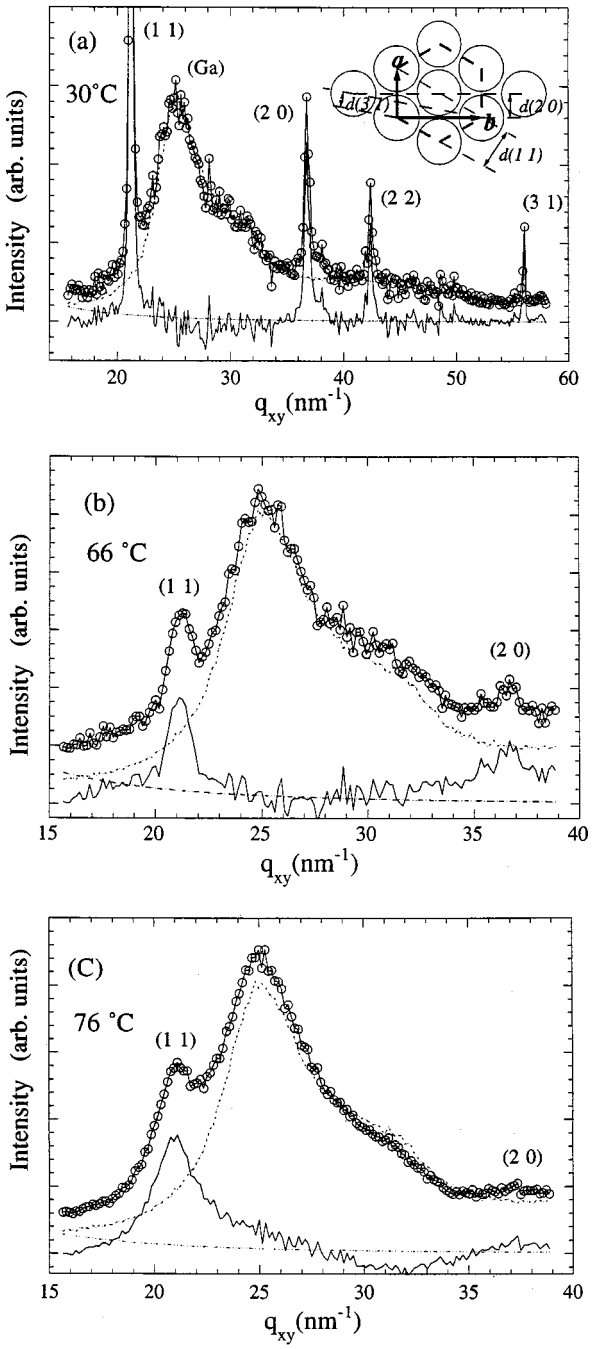

FIG. 8. Grazing-incidence x-ray diffraction from the liquid-vapor interface of dilute PbGa alloys. (a) Observed diffraction pattern at 28 °C. This figure also shows the background scattering from Ga, the stray scattering, and the resultant GIXD pattern after subtraction of the Ga and stray scattering. (b) The GIXD pattern 66 °C. (c) The GIXD pattern at 76 °C.

the average ordered domain size in the samples studied, can be much larger than some tens of nanometers. However, we are not able to obtain a precise value of the correlation length from the data available. In qualitative support of this inference we note that it is difficult to record all of the observed diffraction peaks in one GIXD scan, and the relative intensities of these peaks change irregularly from scan to scan. These observations are consistent with the existence of an inhomogeneous distribution of orientations of large two-dimensional crystalline domains in the Pb monolayer.

Although the x-ray reflectivity measurements imply that the excess Pb in the liquid-vapor interface of the alloy forms a monolayer, those measurements are not sensitive to the presence or absence of a minute number of very small crystals of bulk Pb. To confirm that the observed GIXD patterns arise from a two-dimensional ordered array of Pb atoms, and not from bulk crystals of Pb, we carried out two tests.

One test is based on carrying out scans of the (11) peak with fixed angle of incidence (α) and several different detector pick-off angles (β). The variation of detector angle is equivalent to scanning along q_z. With the angle of incidence fixed at 0.1°, the diffracted x rays were collected at angles between 0.1° and 4.5°. If the (11) peak arises from diffraction from a bulk crystal its position must satisfy the condition $q_{xy}^2+q_z^2=\text{const}$, which implies that the peak position will shift to smaller q_{xy} as q_z increases. If, on the other hand, the (11) peak arises from diffraction from a two-dimensional crystal, its position satisfies the condition $q_{xy}=\text{const}$, and is independent of q_z. Consequently, a measurement of the shift in position of the (11) peak as a function of q_z will distinguish between diffraction from two-dimensional and three-dimensional crystals. As shown in Figs. 9(a) and 9(b), the position of the (11) peak does not depend on the value of q_z. The same result is obtained from a study of the position of the (20) peak as a function of q_z [see Fig. 9(c)].

A second test is based on measurement of the intensity of the (11) diffraction peak as a function of q_z. Over the range of detector pick-off angle we used, $0<\beta<4.5°$, there would be no change in the intensities of the diffraction peaks from a two-dimensional crystalline Pb monolayer that exhibits no roughness. Our fits to the reflectivity data imply that the Pb monolayer has a small, but nonzero, roughness, which we account for with a Debye-Waller factor. Then, we expect that the intensity as a function of q_z is damped as $\exp(-\sigma_{\text{Pb}}^2 q_z^2)$. Figure 10(a) displays the results of several such measurements. We found that in any particular scan sharps peaks (with widths much smaller than the instrumental resolution of the q_z scan) may occur; the intensities and the positions of these peaks vary irregularly from one scan to another. The intensities of the peaks vary, apparently randomly, on a time scale of ten or more seconds. These observations suggest that the peaks are the signatures of motion of the two-dimensional crystalline domains of the Pb monolayer. As these domains move in the footprint of the x-ray beam, with fixed angle of incidence and fixed q_{xy}, different diffraction conditions are satisfied. If this supposition is correct, the true peak intensity can be obtained either from a very long scan or from the superposition of multiple scans carried out on a time scale shorter than the time scale of the intensity variation. The time available at a synchrotron x-ray source, coupled with the small rate of diffusion of two-dimensional ordered domains, makes the latter the method of choice. Figure 10(b) displays the results of averaging 69 scans of intensity versus q_z for the (11) diffraction peak. Comparisons of the measured intensity of the (11) diffraction peak with the theoretical intensities for the (11) diffraction peaks from a monolayer and from a 3D powder indicate that the Pb atoms form a monolayer in the liquid-vapor interface of the alloy [Fig. 10(b)].

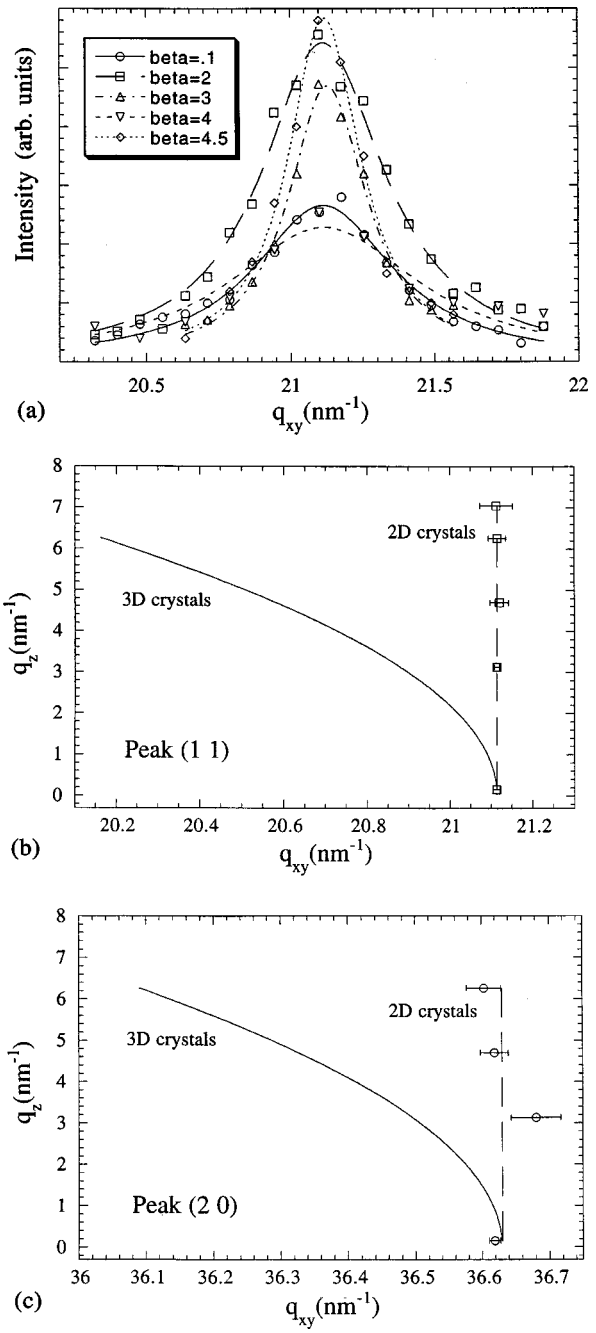

FIG. 9. (a) Scans of the (11) GIXD peak with different detector pick-off angles (β). (b) The position of the center of the (11) diffraction peak as a function of q_z. (c) The position of the center of the (20) diffraction peak as a function of q_z.

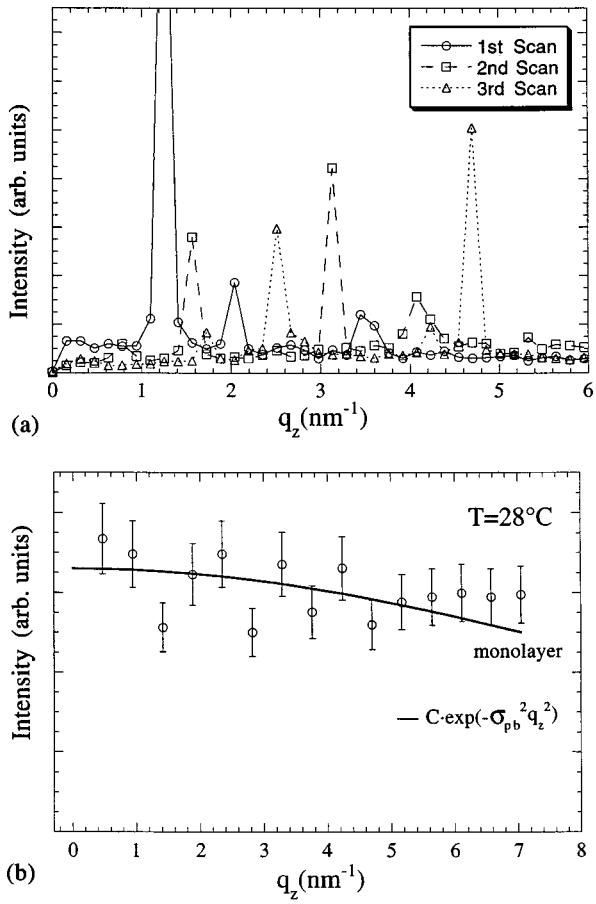

FIG. 10. (a) Three individual β scans of the (11) diffraction peak with fixed 2θ as a function of q_z. (b) The average of 69 β scans of the (11) diffraction peak with fixed 2θ as a function of q_z.

Around 58 °C the GIXD patterns fall into two categories. Sometimes the FWHM's of the (11) and (20) diffraction peaks are small and sensibly equal to our instrumental resolution, and sometimes about five to six times larger. In both kinds of GIXD pattern the positions of the diffraction peaks are the same. Although we have not captured coexistence of narrow and broad diffraction peaks in the same GIXD scan, these results imply that there is a phase transition at about 58 °C, which is the midpoint of the temperature range over which there is an abrupt change in correlation length (see Fig. 11). The FWHM of the (11) diffraction peak in the more ordered phase corresponds to a positional correlation length of at least 25 nm, while the FWHM of the (11) diffraction peak in the less ordered phase corresponds to a positional correlation length of about 4 nm. The apparently discontinuous change in the positional correlation length across the transition suggests that it is first order.

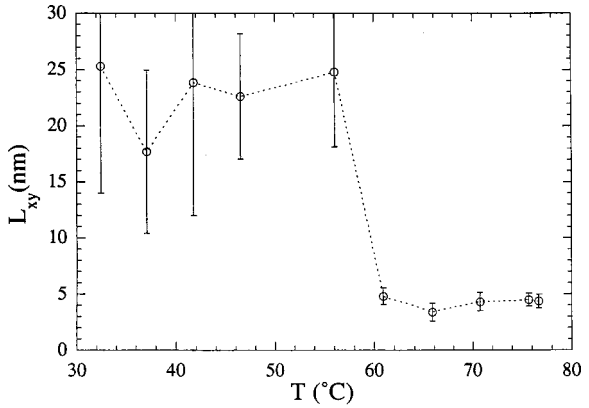

FIG. 11. Translational correlation length as a function of temperature, obtained from deconvolution of the observed (11) reflection peak with the instrument resolution function. The instrumental resolution function corresponds to $L = 28$ nm.

IV. DISCUSSION

Our observations lead to the following three inferences: (1) The excess Pb in the liquid-vapor interface of dilute PbGa alloys forms a monolayer that is the outermost stratum of that interface. (2) At temperatures below 58 °C that Pb monolayer forms a two-dimensional hexagonal solid. (3) A first-order solid-to-disordered (liquid or hexatic) phase transition occurs in that monolayer at about 58 °C.

The conclusion that the excess Pb in the liquid-vapor interface of a dilute PbGa alloy forms a monolayer that is the outermost stratum of that interface is supported by the results of self-consistent quantum Monte Carlo simulations reported by Zhao and Rice.[33] The calculated density distribution along the normal to the interface is in good agreement with that inferred from the experimental data.

In our preliminary report of this work[34] we suggested that the less ordered phase cannot be a liquid, since the first- and second-neighbor separations in a liquid are never in the same ratio as in the crystalline solid. However, examination of the pair correlation function of a dense two-dimensional liquid has convinced us that this observation is not relevant. Since we do not have sufficient experimental range in q space to determine the rate of decay of the envelope of the pair correlation function, our data do not determine if the disordered state observed is a liquid or a hexatic. We also note that our experiments do not directly determine the density of the Pb monolayer. Nevertheless, we believe that our inference that the density change across the transition is very small or, possibly, zero, from the observation that the diffraction peak positions are the same in the low- and high-temperature phases, is accurate.

The uncertainty concerning the intervention of a hexatic phase in the melting of the Pb monolayer is also present in Monte Carlo simulations carried out by Chekmarev, Oxtoby, and Rice.[35] Those calculations show that, if a hexatic phase does lie between the ordered solid and the liquid, the density range over which it is stable is extremely small. We note that Celestini, Ercolessi, and Tosatti have suggested, on the basis of the results obtained from simulations using the ''glue model'' Hamiltonian for liquid metals, that the outermost layer of the liquid-vapor interface of a pure metal will exhibit hexatic ordering.[36] These investigators do not report any results concerning the character of the transitions between liquid and hexatic packing, or solid and hexatic packing, in the liquid-vapor interface.

The formation of an ordered monolayer of the excess component segregated in the liquid-vapor interface of an alloy is, to our knowledge, extremely unusual. In the other dilute alloy systems that have been investigated, namely, BiGa,[26,27] SnGa,[28] and InGa,[21] the segregated excess component in the liquid-vapor interface forms a liquid monolayer. Yet, in each of these cases, the temperature at which the alloy was studied is well below the freezing point of the bulk liquid phase of the component in excess in the liquid-vapor interface. It is known that a long-chain amphiphile that is insoluble in water will form an ordered monolayer at the air-water interface, but it is not clear that this observation has any relevance for understanding the behavior of the PbGa alloy. In particular, the liquid-vapor interface of the PbGa alloy supports a two-dimensional crystalline layer of Pb even when the bulk Pb concentration is very far below the solubility limit of Pb in Ga. On the other hand, given that the interface in question does support a two-dimensional crystalline monolayer, the existence of phase transitions within that monolayer is to be expected. For example, a monolayer of long-chain amphiphile molecules supported at the air-water interface is known to undergo several transitions between two-dimensional ordered phases. The only issue is, then, whether the experimental window available includes the temperatures and/or surface densities at which such transitions occur. Apparently, this is the case for the dilute Pb-in-Ga alloys we have studied.

The character of the phase transition in the Pb monolayer is reminiscent of the freezing transition in a two-dimensional one-component plasma. That transition is first order, and it occurs with zero density change (there is a nonzero entropy change). The zero density change across the transition is a consequence of the assumption that the neutralizing jellium background is rigid, whereupon the constraint of electroneutrality requires superposition of the charge densities of the jellium and the mobile component. In our case, the chemical potential of the electrons in the Pb monolayer must be the same as the chemical potential of the electrons in the bulk liquid, which is almost pure Ga. Since the variation of the density of Ga over the temperature range we have studied is very small, we infer that the chemical potential of the electrons in the monolayer corresponds to a system with nearly fixed density. Moreover, since the Fermi temperature of Ga is very high, the chemical potential of the electrons will depend mainly on the electron density and only very weakly on the temperature. Accordingly, we suggest that it is reasonable to expect that the freezing of the Pb ions into a hexagonal lattice will imitate the behavior of a one-component plasma, i.e., occur with zero density change. It is of interest, in this context, that the results of the most recent computer simulations of the crystallization of a classical two-dimensional one-component electron plasma hint, but do not prove, that the two-dimensional crystal phase melts to a hexatic phase.[37]

The formation of a two-dimensional crystalline layer bounding the liquid-vapor interface of liquid Ga should be expected to influence the transverse pair correlation function of Ga in the interface and the longitudinal distribution of Ga atoms across the interface. The signature of the former effect is the appearance of satellite diffraction peaks separated from the diffraction peak of Ga by plus and minus the magnitudes of the reciprocal lattice vectors of the Pb lattice. We do not see such peaks, implying that the interaction between Pb and Ga is very weak. This implication is supported by the calculations of Zhao and Rice.[33] The signature of the latter effect is enhancement of the amplitudes of the density oscillations in the interface relative to the values characteristic of the liquid-vapor interface of pure Ga. A comparison of the fits to the longitudinal density distribution of Ga in the pure Ga liquid-vapor interface and in the liquid-vapor interface of the PbGa alloys shows that the presence of the crystalline Pb monolayer has negligible effect. The implication of this result is that the flexibility of the two-dimensional lattice of Pb atoms is sufficiently great not to measurably constrain the capillary wave excitations of Ga. This inference is supported

by calculations of the reflectivity using model longitudinal density distributions that decay algebraically rather than exponentially. The results of these calculations show that our experimental data do not support enhanced layering of Ga in the liquid-vapor interface of the alloy (the width of the quasi-Bragg peak corresponding to layering along the normal is large enough to preclude extended layering).

ACKNOWLEDGMENTS

This research was supported by a grant from the National Science Foundation (Grant No. CHE-958923). All of the experiments were carried out at station X19C of the National Synchrotron Light Source, Brookhaven National Laboratory.

[1] R. Defay, I. Prigogine, A. Bellemans, and D. H. Everett, *Surface Tension and Adsorption* (Longmans, Green, London, 1966).
[2] M. P. D'Evelyn and S. A. Rice, Phys. Rev. Lett. **47**, 1844 (1981).
[3] M. P. D'Evelyn and S. A. Rice, J. Chem. Phys. **78**, 5081 (1983).
[4] M. P. D'Evelyn and S. A. Rice, J. Chem. Phys. **78**, 5225 (1983).
[5] J. G. Harris, J. Gryko, and S. A. Rice, J. Chem. Phys. **87**, 3069 (1987).
[6] J. G. Harris, J. Gryko, and S. A. Rice, J. Stat. Phys. **48**, 1109 (1987).
[7] A. Gomez and S. A. Rice, J. Chem. Phys. **101**, 8094 (1994).
[8] M. Zhao, D. Chekmarev, Z. Cai, and S. A. Rice, Phys. Rev. E **56**, 7033 (1997).
[9] M. Zhao, D. Chekmarev, and S. A. Rice, J. Chem. Phys. **108**, 5055 (1998); **109**, 1959 (1999).
[10] M. Zhao and S. A. Rice, J. Chem. Phys. **111**, 2181 (1999).
[11] S. A. Rice and M. Zhao, Phys. Rev. B **57**, 13 501 (1998).
[12] S. A. Rice and M. Zhao, J. Phys. Chem. A **103**, 10 159 (1999).
[13] D. Chekmarev, M. Zhao, and S. A. Rice, Phys. Rev. E **59**, 479 (1999).
[14] O. M. Magnussen, B. M. Ocko, M. J. Regan, L. E. Berman, P. S. Pershan, and M. Deutsch, Phys. Rev. Lett. **74**, 4444 (1995).
[15] M. J. Regan, E. H. Kawamoto, S. Lee, P. S. Pershan, N. Maskil, M. Deutsch, O. M. Magnussen, B. M. Ocko, and L. E. Berman, Phys. Rev. Lett. **75**, 2498 (1995).
[16] M. J. Regan, P. S. Pershan, O. M. Magnusen, B. M. Ocko, M. Deutsch, and L. E. Berman, Phys. Rev. B **54**, 9730 (1996).
[17] M. J. Regan, O. M. Magnussen, E. H. Kawamoto, P. S. Pershan, B. M. Ocko, N. Maskil, M. Deutsch, S. Lee, K. Penanen, and L. E. Berman, J. Non-Cryst. Solids **207**, 762 (1996).
[18] M. J. Regan, H. C. Tostmann, P. S. Pershan, O. M. Magnussen, E. DiMasi, B. M. Ocko, and M. Deutsch, Phys. Rev. B **55**, 10 786 (1997).
[19] M. J. Regan, P. S. Pershan, O. M. Magnussen, B. M. Ocko, M. Dentsch, and L. E. Berman, Phys. Rev. B **55**, 15 874 (1997).
[20] E. DiMasi, H. Tostmann, B. M. Ocko, P. S. Pershan, and M. Deutsch, Phys. Rev. B **58**, R13 419 (1998).
[21] H. Tostmann, E. DiMasi, P. S. Pershan, B. M. Ocko, O. G. Shpyrko, and M. Deutsch, Phys. Rev. B **59**, 783 (1999).
[22] E. DiMasi, H. Tostmann, B. M. Ocko, P. S. Pershan, and M. Deutsch, J. Phys. Chem. B **103**, 9952 (1999).
[23] B. N. Thomas, S. W. Barton, F. Novak, and S. A. Rice, J. Chem. Phys. **86**, 1036 (1987).
[24] E. B. Flom, M. Li, A. Acero, N. Maskil, and S. A. Rice, Science **260**, 332 (1993).
[25] E. B. Flom, Z. Cai, A. A. Acero, B. Lin, N. Maskil, L. Liu, and S. A. Rice, J. Chem. Phys. **96**, 4743 (1992).
[26] N. Lei, Z.-q. Huang, and S. A. Rice, J. Chem. Phys. **104**, 4802 (1996).
[27] N. Lei, Z.-q. Huang, S. A. Rice, and C. Grayce, J. Chem. Phys. **105**, 9615 (1996).
[28] N. Lei, Z.-q. Huang, and S. A. Rice, J. Chem. Phys. **107**, 4051 (1997).
[29] The composition of the alloy was determined by atomic absorption spectroscopy (Schwarzkopf Microanalytical Laboratory, Woodside, NY).
[30] L. G. Parratt, Phys. Rev. **95**, 359 (1954).
[31] A. Braslau, P. S. Pershan, G. Swislow, B. M. Ocko, and J. Als-Nielsen, Phys. Rev. A **38**, 2457 (1988).
[32] G. Makov and A. A. Kornyshev, J. Chem. Phys. **104**, 1693 (1996).
[33] M. Zhao and S. A. Rice, Phys. Rev. E (unpublished).
[34] B. Yang, D. Gidalevitz, D. Li, Z. Huang, and S. A. Rice, Proc. Natl. Acad. Sci. USA **96**, 13 009 (1999).
[35] D. Chekmarev, D. Oxtoby, and S. A. Rice (unpublished).
[36] F. Celestini, F. Ercolessi, and E. Tosatti, Phys. Rev. Lett. **78**, 3153 (1997).
[37] S. Muto and H. Aoki, Phys. Rev. B **59**, 14 911 (1999).